REPORT No. 143 S
(S 3/125)

October 1970

NEDERLANDS SCHEEPSSTUDIECENTRUM TNO
NETHERLANDS SHIP RESEARCH CENTRE TNO
SHIPBUILDING DEPARTMENT LEEGHWATERSTRAAT 5, DELFT

★

HULL VIBRATIONS OF THE CARGO-LINER "KOUDEKERK"

(ROMPTRILLINGEN VAN HET LIJNVRACHTSCHIP „KOUDEKERK")

by

IR. H. H. 'T HART
Institute TNO for Mechanical Constructions

Issued by the Council

VOORWOORD

Voor het verifiëren van methoden voor het berekenen van scheepstrillingen zijn betrouwbare gegevens, verkregen door metingen aan boord van schepen, onmisbaar.
Toen dan ook in 1967 de mogelijkheid geboden werd om trillingen te meten aan boord van het m.s. „Koudekerk" werd deze gelegenheid met beide handen aangegrepen.
De metingen werden uitgevoerd door het Instituut TNO voor Werktuigkundige Constructies gedurende een reis naar Zuid-Afrika. Hierbij werd de zogenaamde impedantiemethode toegepast met gebruikmaking van een mechanische excitator.
In dit rapport van deze metingen is speciale aandacht besteed aan de meetmethode, de instrumentatie, de ijking en de interpretatie van de resultaten.
De resultaten zelf zijn gepresenteerd in de vorm van admittantiediagrammen en trillingsvormen voor de resonantiefrekwenties.
De verkregen meetresultaten zijn gebruikt voor twee theoretische studies uitgevoerd door Ir. S. Hylarides (N.S.P.) die resulteerden in twee rapporten getiteld: „Kritische beschouwing van de huidige analysemethoden voor scheepstrillingen" en „Analyse van scheepstrillingen door middel van de elementenmethode. Deel 2", die binnenkort door het Scheepsstudiecentrum zullen worden gepubliceerd.
De waardevolle hulp van de N.V. Vereenigde Nederlandsche Scheepvaartmaatschappij, de eigenares van het schip, wordt met dank vermeld. Ook is dank verschuldigd aan de auteur en alle erbij betrokken medewerkers van het Instituut TNO voor Werktuigkundige Constructies.

HET NEDERLANDS SCHEEPSSTUDIECENTRUM TNO

PREFACE

To verify methods for the calculation of ship hull vibrations, reliable data obtained from full scale measurements are indispensable. Therefore when in 1967 the possibility arose to measure vibrations on board of the m.v. "Koudekerk" this opportunity was seized with both hands.
The measurements were carried out by the Institute TNO for Mechanical Constructions, during a voyage to South Africa. Use was made of the so-called impedance measuring procedure with the application of a mechanical exciter.
In this report on these measurements special attention has been paid to the measuring method, the instrumentation, the calibrations ant the interpretation of the results.
The results itself are presented in mobility diagrams and modal profiles for the resonance frequencies.
The data obtained have been used in two theoretical studies executed by Ir. S. Hylarides (Netherlands Ship Model Basin) and resulting in two reports: "Critical consideration of present hull vibration analyses" and "Ship vibration analysis by finite element technique. Pat 2", that will be published shortly by the Ship Research Centre.
The valuable assistance rendered by N.V. Vereenigde Nederlandsche Scheepvaartmaatschappij, owners of the vessel, is gratefully acknowledged. Also thanks are due to the author and all staff concerned of the Institute TNO for Mechanical Constructions.

THE NETHERLANDS SHIP RESEARCH CENTRE TNO

CONTENTS

LIST OF SYMBOLS

f	frequency	Hz
g	acceleration of gravity	$m \cdot s^{-2}$
k	stiffness	$N \cdot m^{-1}$
m	mass	kg
n	number	
r	radius	m
t	time	s
y	amplitude	m
C	exciter constant	$N \cdot s^2$
M	equivalent mass	kg
P	force	N(ewton)
Q	resonance factor	
V	voltage	V(olt)
$\mathcal{M}$	mobility	$m \cdot s^{-1} \cdot N^{-1}$
α	angle	radian
β	fraction of critical damping	
η_i	relative amplitude with respect to point i	
μ	mass per unit of length	$kg \cdot m^{-1}$
ω	angular frequency	s^{-1}
ω_0	natural frequency $= \sqrt{k/M}$	s^{-1}
Ω	relative angular frequency $= \omega/\omega_0$	

Note 1: The acceleration of gravity g is taken to be 9.81 ms^{-2}

Note 2: In this report units of the SI-system are used. In this system kg is the unit of mass and N (newton) is the unit of force. 1 N $\triangleq$ $1/g$ kgf

HULL VIBRATIONS OF THE CARGO-LINER "KOUDEKERK"

by

Ir. H. H. 't HART

Summary

For the cargoliner "Koudekerk" some natural frequencies of the horizontal and vertical vibration of her hull and the pertinent modal profiles, were determined. The hull was excited by a mechanical exciter. The vibration mode of a section of the double bottom was investigated at two natural frequencies of the hull. This report also compares the results of measurements with those of some calculations of mechanical impedance.

1 Introduction

The measurements described in this report were carried out on board the dry-cargo-liner m.v. "Koudekerk" during one of her voyages from Amsterdam to Cape-Town in 1967. The purpose of the measurements was to determine the dynamic characteristics of the ship in terms of horizontal and vertical vibrations, making use of the impedance measuring method. When this method is applied, exact knowledge of the exciting force as well as of the velocities of the vibrations is essential. Whereas the exciting forces of the propeller and of the main engine were not sufficiently known, the ship was excited by a mechanical exciter and the exciting forces were measured.

The said method of excitation, however, requires an electronic measuring system, which distinguishes between vibrations introduced by the exciter and vibrations introduced by the propulsion system. The present paper describes the measuring procedure, the instrumentation, the calibrations and the measuring results. The results are presented in graphs and figures, and evaluated in order to obtain damping factors and equivalent masses. The equivalent masses are computed from the modal profiles and from the mobility diagrams.

For the main particulars of the m.v. "Koudekerk" see table I.

Table I. Main particulars

Length overall	164.95 m
Length between perpendiculars	152.40 m
Breadth moulded	21.03 m
Depth to upper deck	11.89 m
Summer draught	
as an open shelterdecker	8,00 m
as a closed shelterdecker	8,91 m
Deadweight	
as an open shelterdecker	9940 metric tons
as a closed shelterdecker	12200 metric tons
Service speed	20 knots

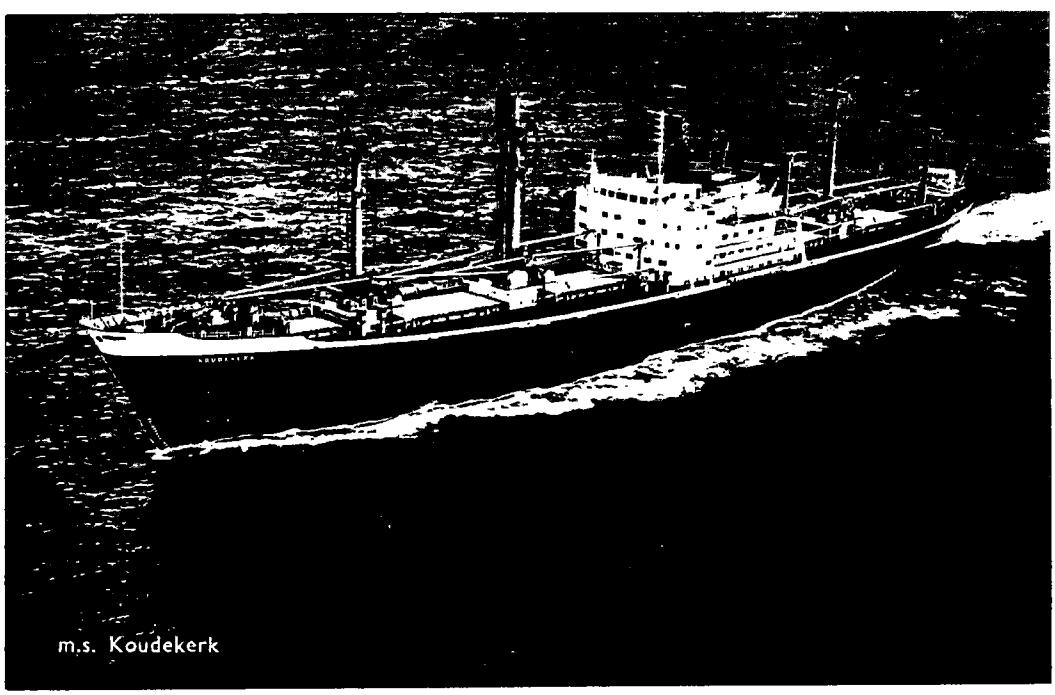

Fig. 1.
m.v. "Koudekerk" at sea.

Courtesy N.V. Vereenigde Ned. Scheepvaartmaatschappij

2 Description of instrumentation

2.1 *Exciter*

Figure 2 shows the principle of the mechanical exciter used. The two heavy wheels are each provided with an unbalance mass m at a radius r. The flywheels are coupled in such a way that they turn, at the same speed, in mutually opposite directions. The unbalance forces are equal, so that:

$$m_1 r_1 = m_2 r_2 = \tfrac{1}{2} mr$$

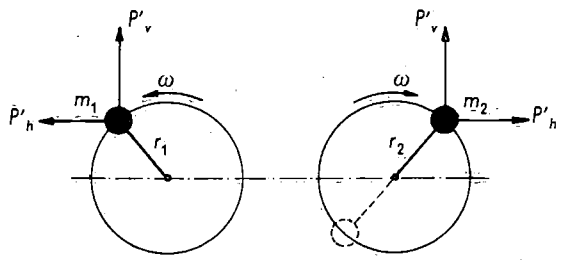

Fig. 2. Principle of the mechanical exciter.

In case the masses m_1 and m_2 are fixed to the flywheels, as shown in Figure 2, a free force in vertical direction is excited:

$$P_v = 2P'_v = mr\omega^2 \sin \omega t$$

while

$$P_h = 0$$

Unbalance mass m_2 can be fixed to the flywheel with a phase shift of 180 degrees. This situation is represented by a dotted line. Then:

$$P_v = 0$$

$$P_h = 2P'_h = mr\omega^2 \sin \omega t$$

The flywheels reduce the variations of the angular velocity of the exciter to a negligible amount, even at a low running speed of 1.5 Hz and with maximum unbalance masses. Besides, this problem occurs only at vertical excitation. During horizontal excitation, the driving and breaking moments are in constant equilibrium. Using a 20 HP adjustable three-phase motor, each frequency wanted from 1.5 Hz up to 10 Hz could be adjusted and kept constant. The frequency variations were less than 0.5 per cent of the adjusted value.

The excitation force can be adjusted at a large number of values by placing more or fewer unbalance masses on the flywheels. Actually, there are 16 possibilities, numbered A to R. At each adjustment, the value of $m \cdot r$ is constant. This constant is called C_A to C_R. The amplitude of the exciting force must be calculated from:

$$P = C \cdot \omega^2 \quad \text{N RMS (Newton- Root Mean Square)}$$

Table II lists the values of constants C which were used during the measurements under report.

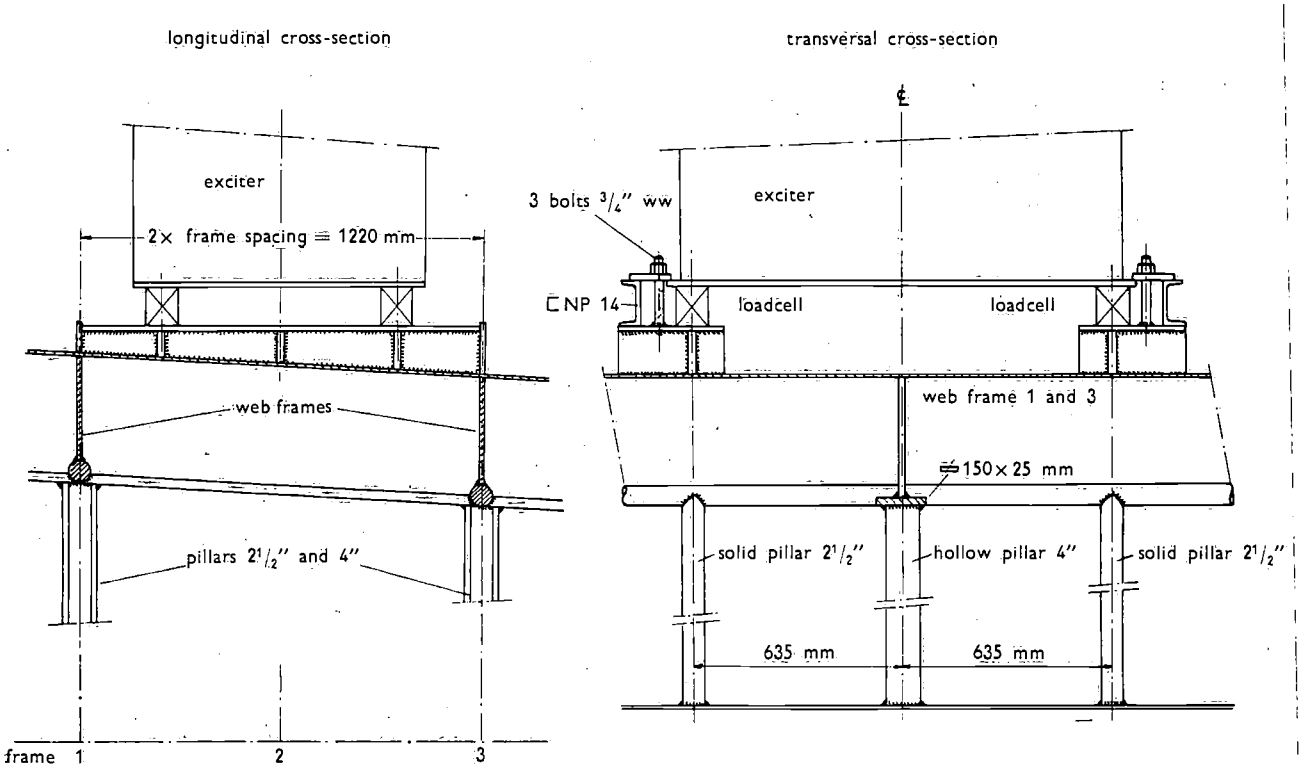

Fig. 3. Exciter foundation m.v. "Koudekerk".

Table II. Constants C in Nsec² for different excitation levels •

C_A	C_B	C_C	C_E	C_H
87.845	58.558	43.923	20.415	7.2663

The exciter designed for a maximum exciting force of 35,000 N amplitude RMS, was placed in hold VI on a special foundation between frames 1 and 3. The deck was supported by 6 pillars, which were founded upon the floors in the after peak tank. The situation is shown in figure 3. The exciter itself was placed on four loadcells, which were prestressed by four anchor bolts. In principle the clamping construction is staticly undetermined. The exciting force is transferred to the foundation partly through the bolts and partly through the loadcells. In order to keep the contribution of the bolts as small as possible – and to unload the bolts dynamically – dish springs were applied underneath the nuts. The complete clamping construction is shown in figure 4. The loadcell has a facility to level the exciter and to adjust the prestress. The exciter was fixed in horizontal direction by means of four tie bolts.

The way of measuring and calibrating the vertical and horizontal exciting forces is described in paragraph 2.3.

2.2 *Vibration pick-ups*

The vibrations were measured with accelerometers. This type of vibration pick-up is very suitable for the purpose of measuring vibration amplitudes at low frequencies, especially in the frequency range from 1.5 Hz to 10 Hz which is under consideration, because of their linear characteristics. However, the accelerometer is also sensitive to the ship's motions caused by

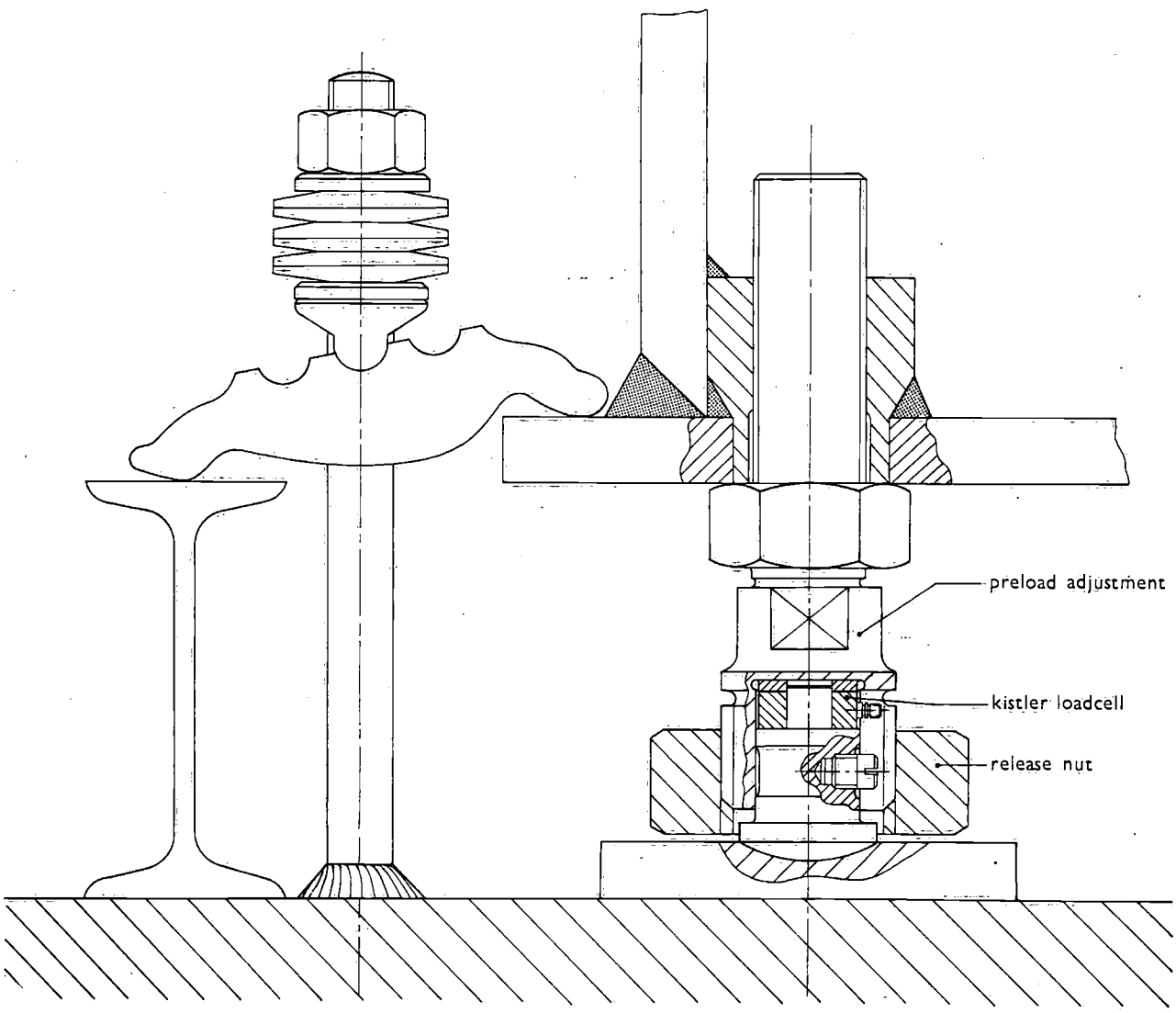

Fig. 4. The clamping construction.

seawaves. The ship's accelerations due to seawaves are of the same order of magnitude as the accelerations excited by the vibration exciter. They can extend to much higher values during rough sea conditions. This disadvantage was eliminated by use of an electronic filter.

Another property of the accelerometer is its sensitivity to noise. Every mechanical vibration with relatively high frequencies from unknown sources is, in this context, called noise. This unwanted effect was eliminated, as far as possible, by using accelerometers with low resonance frequencies. Actually, two types of accelerometers were applied.

The largest pick-ups with the lowest resonance frequency were applied in the measuring places wich were easily accessible. The specification is as follows:

Make	TNO
Measuring system	inductive
Range	0.7*g*
Resonance frequency	20 Hz nominal
Sensitivity	200 scale units per *mg* in combination with Hottinger amplifier
Dimensions	H 180, groundplate 190 × 190 mm

The following type of accelerometer was used in the measuring places where small dimensions were required:

Make	Statham
Type	A5-2.5-350 and A69TC-5-350
Measuring system	strain gauge
Range	2.5*g* and 5*g*
Resonance frequency	110 Hz nominal and 375 Hz nominal
Sensitivity	5 mV/V at full scale
Dimensions	H 64 mm

Six items of each Statham type accelerometer were available. They were glued to the tank top in hold III. In all the other measuring places, i.e. on deck near the exciter and in the holds, a TNO accelerometer was used, each meter was placed on the wanted location by hand and adjusted, horizontally or vertically, by three adjusting screws in the base plate. By means of four lead measuring cables, the 6 pick-ups were connected with the measuring amplifiers, which had been accommodated in the mate's office.

2.3 *Measuring equipment*

Figure 5 gives a block diagram of the measuring installation. Four measuring systems are built together.

2.3.1 Measuring of exciting force

The exciter is mounted on four piëzo-electric load cells. The four outputs are fed to four charge amplifiers. The outputs of the amplifiers are added. The

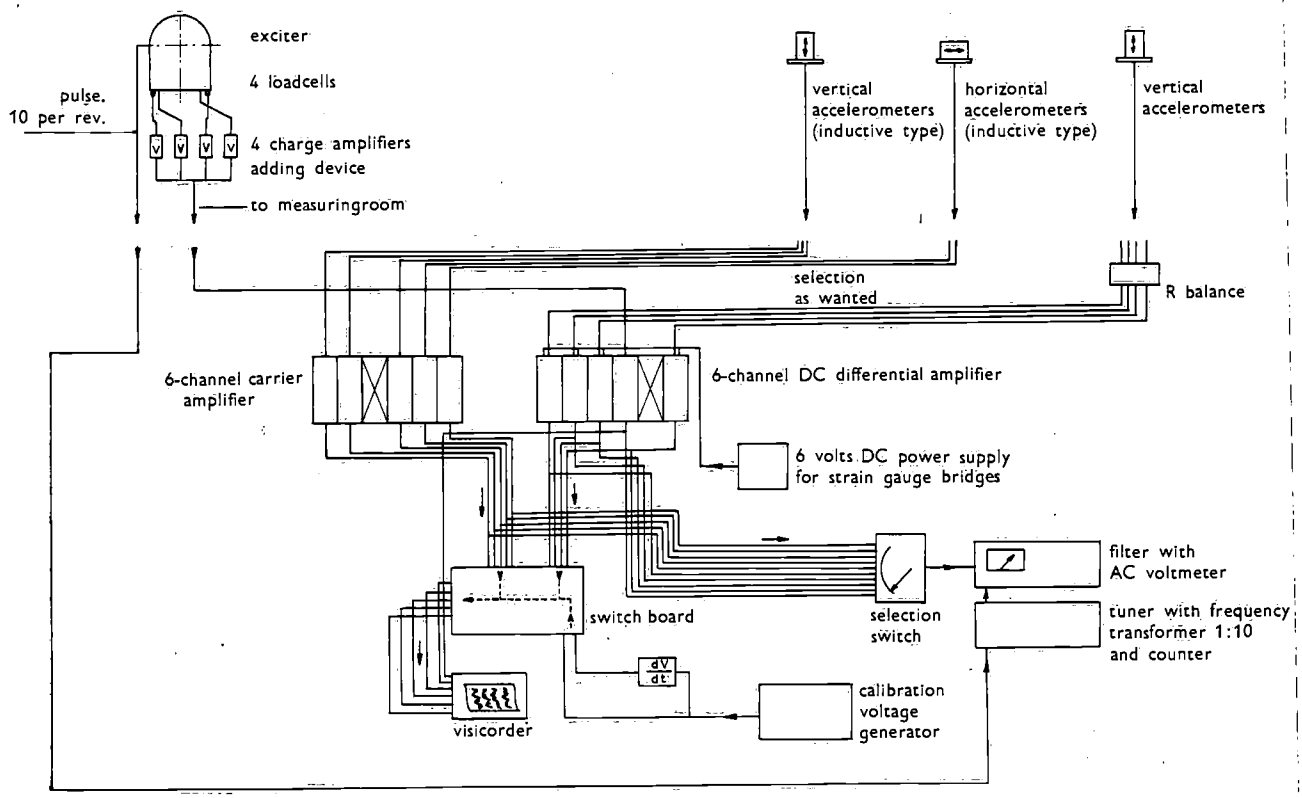

Fig. 5. Block diagram of the measuring installation.

sum-signal is amplified again by a DC-amplifier, and fed to the recording and reading sections of the installation.

2.3.2 Inductive system

The TNO accelerometers of the inductive type are connected to a six channel inductive measuring amplifier. The outputs are directly connected with the recording and reading sections.

2.3.3 Strain gauges

The strain gauge bridges of the 12 accelerometers in hold III are excited by 5 V DC from a power supply unit. The output signal of the bridge is amplified 1,000 times by means of a differential amplifier. Since only four amplifiers were available, and 12 accelerometer signals presented, a channel selector was applied. This selector is provided with a balancing device for each measuring channel. The amplifiers are connected with the recording and reading sections.

2.3.4 Device for measuring frequency

The exciter is provided with a magnetic pick-up, which produces ten pulses at each revolution of the exciter. The exciting frequency is measured by counting the pulses with an electronic counter. The pulse train is used also in the reading section of the installation, which will be discussed below.

2.3.5 Recording and reading section

All amplifier outputs are connected with a selection switch board, from which a selection of five measuring signals is recorded on a multichannel oscillograph for the sake of general control and for measuring the mutual phase relations. By way of a selection switch, the amplifier outputs are also fed to an electronic filter with a band width of 2 Hz constant. The centre frequency of the filter is tuned by a sine generator. Thanks to the pulse train from the exciter (10 times per revolution) and a frequency divider (10 to 1), the oscillating frequency – and therefore the filtered frequency – is identical with the exciting frequency. The filtered output is read from an AC meter.

3 Measuring procedure

All measuring results mentioned in this paper are based on readings during measurements, from the AC voltmeter. Two types of measurement are reviewed in 3.1 and 3.2.

3.1 *Resonant frequency*

In a number of selected measuring points, acceleration amplitudes were measured as a function of frequency. The number of revolutions of the exciter was increased by steps of 0.05 Hz nominal. At each constant frequency, the following data were collected:

excitation force amplitude	P
frequency	f
acceleration amplitude	$\ddot{y}_i$

Since the mobility measuring technique was applied, the wanted value for each measuring point was found to be:

$$\left|\mathcal{M}\right| = \left|\frac{\dot{y}_i}{P}\right| \text{ or } \left|\mathcal{M}\right| = \left|\frac{\ddot{y}_i}{\omega \cdot P}\right| = \left|\frac{\ddot{y}_i}{2 \cdot \pi \cdot f \cdot P}\right|$$

At each adjusted frequency, value $|\mathcal{M}|$ was calculated from the meter readings.

3.2 *Modal profile*

At a number of selected frequencies, acceleration amplitudes in more than 40 locations were measured. The amplitudes were calculated with respect to the amplitude in a reference point, thus:

$$\eta_i = \frac{\ddot{y}_i}{\ddot{y}_{\text{ref}}}$$

Since the readings were done at a constant frequency, the relative accelerations were identical to the relative displacements, thus:

$$\eta_i = \frac{y_i}{y_{\text{ref}}}$$

When the phase relation between the amplitude in the measuring points and the amplitude in the reference point is taken into account, we called the plot of η_i the modal profile. When the phase relations are unknown or uncertain, the absolute value of η_i was plotted; the result we called "transfer function".

4 Calibrations

The results of the resonant frequency measurements are presented in velocity per unit of excitation force, or

$$\left|\mathcal{M}\right| = \left|\frac{b \cdot q}{a \cdot p}\right| \frac{1}{\omega} = \left|\frac{b}{a}\right| \cdot \frac{q}{p} \cdot \frac{1}{\omega}$$

where

a = meter reading "force"
b = meter reading "acceleration"
p = calibration factor "force"
q = calibration factor "acceleration"

The absolute accuracy of the results depends on the ratio of the two calibration factors, q/p. The relative and absolute error of the angular frequency can be neglected, because the frequency was measured with a period counter with 5 digits. In the following sections we will consider the calculation of factors p and q.

4.1 *Calibration accelerometers of (factor q)*

An accelerometer measuring system can be calibrated by turning the meter a known angle around a horizontal axis. The 12 accelerometers in hold III were calibrated in this way by turning them 180 degrees, this being equivalent to an input of $2g$. The output of the strain gauge measuring system is linearly dependent on the excitation voltage. Therefore, the calibration factors of the pick-ups are basically presented in: V/V per g. Actually, the excitation voltage was 5 V DC and the amplification factor of the differential amplifiers was 1,000. The calibration factors of the complete measuring system, which appear in table A-I of Appendix A, are based on these figures. The accelerometers had to be calibrated before they were mounted on the tank top. In view of the time difference between calibration and measurements, an accuracy of $\pm$ 2% can only be guaranteed.

The inductive accelerometers have a range of $\pm$ 0.7g. They cannot be turned upside down. We used a special unit, on which the accelerometer can be turned round a horizontal axis 11½ degrees in both directions. According to figure 6, the input of the horizontally sensitive pick-up is:

$$\text{input hor.} = OB = g \cdot \sin\alpha = 200mg$$

For the vertically sensitive accelerometer holds:

$$\text{input vert.} = OC - OA = g \cdot (1 - \cos\alpha) = 20mg$$

Both values have an absolute accuracy lower than $\pm$ 1%. During calibration, the amplifier output was compared with the mg input. So the sensitivity and the accuracy of the amplifier is included in the results of the calibrations. The amplifier outputs, converted to a constant input of 200mg and a constant sensitivity of the amplifiers, measured during a number of readings with the aid of an accurate digital voltmeter, are listed in table A-II of Appendix A. For each accelerometer, the average value of the readings is given together with the standard deviation, which is defined as:

$$\sigma = \frac{\sqrt{\frac{(x-\bar{x})^2}{n-1}}}{\bar{x}} \cdot 100^0/_0$$

The standard deviation of accelerometer G_2 (9%) is very large. This is due to the fact that the sensitive measuring system is not mounted exactly perpendicular to the groundplate. The misalignment is about 20 arc-minutes. We call this deviation δ. The static calibration in one direction is:

$$1 - \cos(\alpha + \delta) = 1 - \cos(11°30' + 20') = 1 - \cos 11°50'$$

And in the other direction: $1 - \cos 11°10'$

So, the "g" inputs to the system are 21.2mg and 18.9mg respectively in stead of 20mg.

The averaged "g" input is:

$$\frac{1 - \cos(\alpha+\delta) + 1 - \cos(\alpha-\delta)}{2} = 1 - \cos\alpha \cdot \cos\delta =$$

$$= 1 - 0.99996 \cos\alpha$$

In spite of the fact that the standard deviation of the readings of G_2 is very large, the averaged value of the readings may be considered to be the right value with far more accuracy. Due to the ship's motions it was impossible to elaborate these calibrations at sea. Taking into account the time difference between the calibrations in our laboratory and the measurements we give the accuracy of the calibration factors of the inductive accelerometers as $\pm$ 5%.

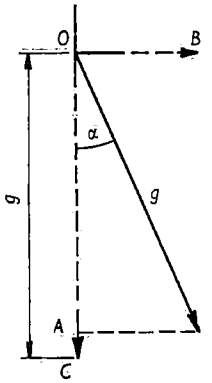

Fig. 6.

4.2 *Calibration of force (factor p)*

Calibration of the force measuring system was based on the design data of the vibration exciting machine, which are listed in table II. The calculated exciting force amplitude was compared directly with the meter readings at a large number of frequencies. This was done for each excitation level and for each excitation direction. The results of these calibrations are listed in tables A-III and A-IV of Appendix A. The average values and the standard deviations were calculated; they are shown in the same tables. The standard deviation was found to be rather large. However, the num-

ber of readings was such that, with favourable result, the mean deviation of the mean could be calculated. This deviation was found to be smaller than 1%. Therefore, the calibration factor of the force is considered to be better than ± 1%.

The calibration procedure described above is the most accurate one; there is no reliable alternative. Computing the calibration factor from the data of loadcells, charge amplifiers, adding device and amplifier is too uncertain.

The calibration factor for horizontal excitation was found to differ from the calibration factor for vertical excitation. During vertical excitation, all four force meter signals were in phase and the four signals were added. During horizontal excitation, the starboard forces were found to be in counterphase with the portside forces. Adding all signals would thus have resulted into a zero output. Therefore, during horizontal excitation only two forcemeters were connected with the measuring system. The relation between the horizontal free force and the vertical reaction on the foundation at one side of the exciter was determined by the dimensions of the exciter and by those of the clamping construction.

5 Measuring results

5.1 *Weather conditions*

An abstract from the meteo reports of 12.00 a.m. is given in table A-V of Appendix A. It appears that the weather conditions during the voyage were extremely good. The ship's motions were very moderate indeed, especially on August 8, 9 and 10, when the ship sailed before the wind. More to the South, the weather conditions gradually worsened. On August 17th they were such that measurements were impossible. However, by that date the measurements had been completed and the instruments were packed.

All in all the weather conditions hardly affected the measurements.

5.2 *Measuring programme*

The measurements, which have been evaluated from the voltmeter readings, are listed below. For the sake of simplicity, all measurements which are of no interest within the scope of this report, are omitted. (MP means measuring point).

Series I

Resonant frequency measurement during vertical excitation.

MP 1, vertical
MP 17, vertical
MP 30, hold III, vertical
} see fig. 7

Ranges:

1.34–2.56 Hz, excitation constant C_A, date: August 6th
2.90–4.39 Hz, excitation constant C_C, date: August 7th
4.26–6.36 Hz, excitation constant C_E, date: August 7th
6.42–8.55 Hz, excitation constant C_H, date: August 8th
8.45–9.95 Hz, excitation constant C_H, date: August 9th

When measuring from 6.42 to 8.55 Hz, the speed of the main engine was reduced to 80 rpm. At 114 rpm the frequency of the 4th order vibration was found to be 7.6 Hz.

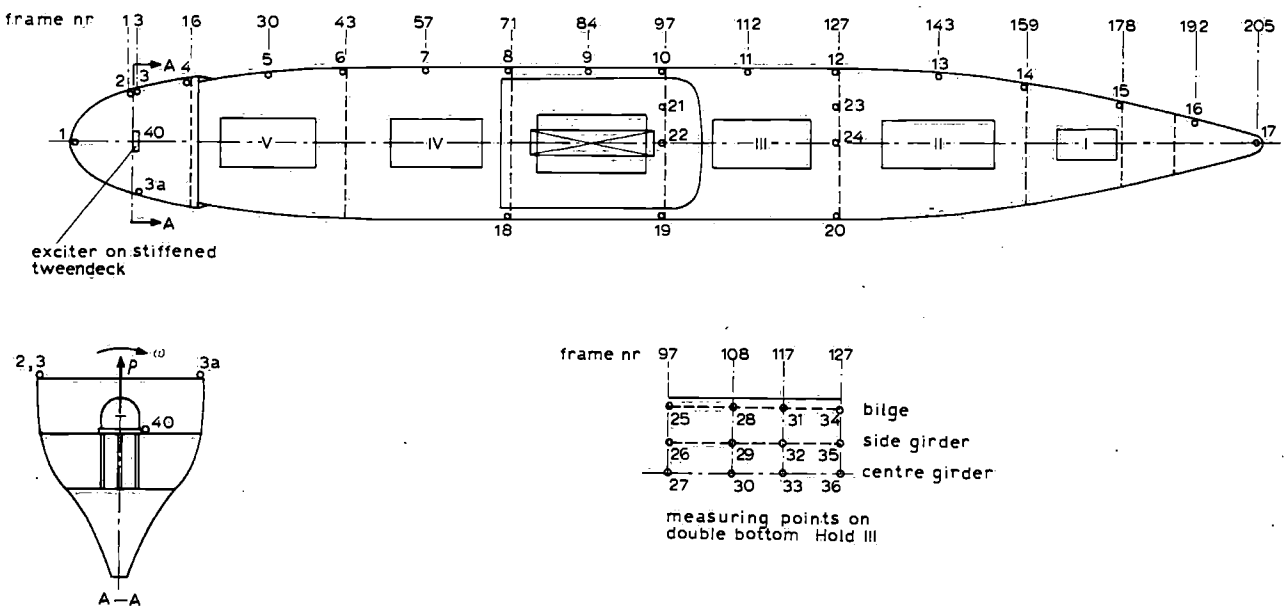

Fig. 7. Measuring points m.v. "Koudekerk".

Series II
Modal profile measurement, vertical excitation.

MP 1 through 36, vertical

Frequencies:

4.25 Hz, constant C_E, MP 1 through 20, 23, 24, date: August 7th
2.46 Hz, constant C_A, MP 1 through 20, 23, 24, date: August 8th
3.34 Hz, constant C_C, MP 1 through 36, date: August 9th
2.46 Hz, constant C_E, MP 21, 22, 25 through 36, date: August 9th
4.25 Hz, constant C_A, MP 21, 22, 25 through 36, date: August 9th

The measuring points appear in figure 7.

Series III
Resonant frequency measurement during horizontal excitation.

MP 17, athwartships
MP 40, athwartships
MP 3, vertical
MP 3a, vertical
} see figure 7

Ranges:

3.00–4.43 Hz, excitation constant C_C, date: August 10th
4.23–6.51 Hz, excitation constant C_E, date: August 10th
6.50–9.00 Hz, excitation constant C_H, date: August 11th
1.44–2.43 Hz, excitation constant C_B, date: August 12th

During the last measurement in the range from 1.44–2.43 Hz the engine speed was 95 rpm. At 114 rpm, the ship's hull was found to be excited in one of its natural frequencies.

Series IV
Modal profile measurements, horizontal excitation.
MP 1 through 24, all vertical and athwartships.

Frequencies:

3.99 Hz, constant C_C, MP 1 through 24, date: August 11th
3.52 Hz, constant C_C, MP 1 through 24, date: August 11th
1.96 Hz, constant C_B, MP 1 through 17, date: August 12th

The measuring points appear in figure 7.

During the measurement at 1.96 Hz the engine speed was reduced to 96 rpm.

5.3 *Results*

The mobility diagrams appear in the diagrams B-1 through B-6 of Appendix B. The modal profiles and the transfer functions are given in diagrams B-7 and B-8. The main results are summarized in table III.

Table III. Measured natural frequencies

vertical vibration modes	horizontal vibration modes	torsional vibration modes
3 nodes 2.46 Hz	2 nodes 1.96 Hz	1 node 3.99 Hz
4 nodes 3.34 Hz	3 nodes 3.99 Hz	
4 nodes 4.15 Hz		

The 4-noded vertical vibration mode was found at two frequencies. In this connection the vibration mode of the section of the double bottom in hold III is of great interest. The double-bottom vibrations were measured at the three vertical natural frequencies of the hull, and are presented in diagram B-9. The amplitudes are the largest at 3.34 Hz. It should be noted that in hold III the double-bottom, loaded with the cargo was found to have a resonant frequency close to 3.34 Hz. We will return to this point in section 6.

6 Interpretation

We will restrict ourselves to the ship's vertical vibrations during vertical excitation; interpretation of horizontal vibrations is far more difficult because of the coupling between horizontal and torsional vibrations. Since the "Koudekerk" is symmetrical in the vertical plane, and its hull is excited in the centre line, horizontal and torsional vibrations during vertical excitation can, and will, be neglected.

Close to the natural frequencies, the characteristics of the hull get very near to the simple mass-spring-damping system with one degree of freedom. In what now follows, an effort is made to find the dynamic constants of the equivalent mass-spring systems of the hull at the three natural frequencies measured.

The mobility of one-degree-of-freedom system is given by

$$\mathcal{M} = \frac{\Omega}{\sqrt{kM}} \frac{1}{\sqrt{(1-\Omega^2)^2+4\beta^2\Omega^2}}$$

(For derivation see Appendix C-I)

The maximum value of $\mathcal{M}$ appears at resonance ($\Omega = 1$)

$$\mathcal{M}_{max} = \frac{1}{2\beta\sqrt{kM}}$$

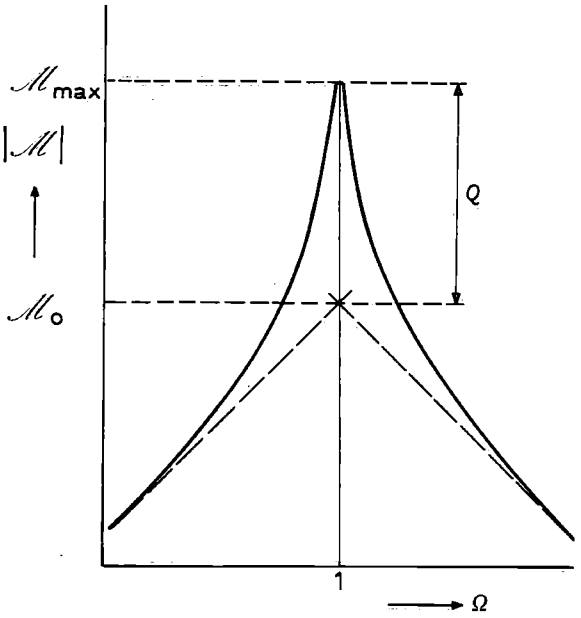

Fig. 8. Mobility diagram of a one-degree-of-freedom system. (logarithmic scales)

The mobility diagram of a one-degree-of-freedom system appears in figure 8. There are two asymptotes.

The intersection of the two asymptotes is called $\mathcal{M}_0$. The mobility in this point is:

$$\mathcal{M}_0 = \frac{1}{\omega_0 M} = \frac{\omega_0}{k} = (\sqrt{kM})^{-1}$$

and

$$\frac{\mathcal{M}_{max}}{\mathcal{M}_0} = \frac{1}{2\beta} = Q$$

We introduce p: $\mathcal{M} = p\mathcal{M}_{max}$, with $p < 1$, so that

$$\frac{p}{2\beta} = \frac{\Omega}{\sqrt{(1-\Omega^2)^2+4\beta^2\Omega^2}}$$

After evaluation of this equation and neglecting β^2 with respect to the unit, we obtain

(see Appendix C-II)

$$\frac{\Delta\omega}{\omega_0} = 2\beta\sqrt{\frac{1}{p^2}-1},$$

where $\Delta\omega$ is the "width" of the resonance peak

For instance, with

$$p = \tfrac{1}{2}\sqrt{2} \qquad \frac{\Delta\omega}{\omega_0} = 2\beta$$

and

$$p = \tfrac{1}{2} \qquad \frac{\Delta\omega}{\omega_0} = 2\beta\sqrt{3}$$

So, once damping factor β is known from the "width" of the resonance peak, point $\mathcal{M}_0$ can be found and the mass and stiffness of the equivalent system calculated.

The above method of calculation is now applied to the mobility diagrams B-1 and B-2. The calculated damping factors are listed in table IV.

Table IV. Calculated damping factors.

	measuring point 1		measuring point 17	
natural frequency	β	Q	β	Q
2.46 Hz	1.2%	42	1.2%	42
3.34 Hz	3.4%	15	2.3%	22
4.15 Hz	3.2%	16		

The damping at the higher frequencies is larger than at the lowest frequency. We expect that at even higher frequencies the damping is such that hardly any resonance peak will occur. The results actually measured point in the same direction.

The equivalent masses are calculated; they are given in table V. Each mass only holds for the measuring point at which the mobility was measured.

Table V. Calculated equivalent mass

	equivalent mass kg	
natural frequency	measuring point 1	measuring point 17
2.46 Hz	$1.9 \cdot 10^6$	$2.4 \cdot 10^6$
3.34 Hz	$3.8 \cdot 10^6$	$3.1 \cdot 10^6$
4.15 Hz	$1.6 \cdot 10^6$	–

The equivalent masses in table V are based on the mobility diagrams for measuring points 1 and 17, while the excitation force was applied in measuring point 40. This type of mobility is called transfer mobility. The equivalent masses are not the equivalent mass of the ship's hull. The equivalent mass of the hull can only be found from the driving point mobility, which is not measured. However, with the aid of a reasonable assumption the driving point mobility in point 40 can be found and the equivalent mass of the hull in point 40 (M_{40}) can be calculated.

We already found:

$$\mathcal{M}_0 = \frac{1}{\omega_0 M} = \frac{\mathcal{M}_{max}}{Q},$$

so for measuring point 1 holds:

$$m_1 = \frac{Q_1}{\mathcal{M}_{max_1}\omega_0}$$

and for measuring point 40:

$$M_{40} = \frac{Q_{40}}{\mathcal{M}_{max_{40}}\omega_0},$$

so that:

$$M_{40} = m_1 \frac{Q_{40}}{Q_1} \frac{\mathscr{M}_{\max_1}}{\mathscr{M}_{\max_{40}}}$$

We take Q_{40} to be equal to Q_1. This is a reasonable assumption because hull vibrations are concerned and measuring points 1 and 40 are located close to each other. The ratio of the maximum values of the mobilities equals the amplitude ratio, so that:

$$\frac{\mathscr{M}_{\max_1}}{\mathscr{M}_{\max_{40}}} = \frac{y_1}{y_{40}} = \frac{1}{\eta_{40}}$$

and

$$M_{40} = m_1 \frac{1}{\eta_{40}}$$

In the same way is found:

$$M_{40} = m_{17} \frac{Q_1}{Q_{17}} \frac{\eta_{17}}{\eta_{40}}$$

Since all values at the right hand side of the two equations are known, M_{40} is calculated in two different ways. The results of these calculations appear in table VI.

Table VI. Calculated equivalent mass of the hull

frequency (Hz)	from measuring point 1			from measuring point 17			
	η_{40}	m_1 (kg)	M_{40} (kg)	η_{17}	$\frac{Q_{17}}{Q_1}$	m_{17} (kg)	M_{40} (kg)
2.46	0.65	$1.9 \cdot 10^6$	$2.9 \cdot 10^6$	0.76	1.0	$2.4 \cdot 10^6$	$2.8 \cdot 10^6$
3.34	0.84	$3.8 \cdot 10^6$	$4.5 \cdot 10^6$	1.58	1.46	$3.1 \cdot 10^6$	$4.0 \cdot 10^6$
4.15	0.66	$1.6 \cdot 10^6$	$2.4 \cdot 10^6$	–	–	–	–

Let us consider the masses M_{40} more closely. The ship's hull is replaced by a one-degree-of-freedom system at each natural frequency. The hull is excited in point 40 and the amplitude in that point is y_{40}. The kinetic energy of the equivalent system should be the same as the kinetic energy of the hull, so that:

$$\tfrac{1}{2} M_{40} y_{40}^2 \omega^2 = \tfrac{1}{2} \int_0^l \mu y^2 \omega^2 \, dx$$

or

$$M_{40} y_{40}^2 = y_1^2 \int_0^l \mu \eta^2 \, dx = y_1^2 M_1$$

and

$$M_{40} = \frac{1}{\eta_{40}^2} M_1$$

The value of M_1 is calculated from the modal profiles, the known distribution of the masses of the ship and the cargo and the estimation of the added water mass; see table VII.

Table VII. Equivalent mass calculated from the modal profiles (in kg)

		natural frequencies			total mass (kg)
		2.46 Hz	3.34 Hz	4.15 Hz	
ship		$0.54 \cdot 10^6$	$1.21 \cdot 10^6$	$0.41 \cdot 10^6$	$6.6 \cdot 10^6$
cargo		$0.32 \cdot 10^6$	$0.79 \cdot 10^6$	$0.20 \cdot 10^6$	$7.1 \cdot 10^6$
added water		$0.46 \cdot 10^6$	$0.87 \cdot 10^6$	$0.34 \cdot 10^6$	–
total	M_1	$1.32 \cdot 10^6$	$2.87 \cdot 10^6$	$0.95 \cdot 10^6$	–
	η_{40}	0.65	0.84	0.66	–
	M_{40}	$3.12 \cdot 10^6$	$4.06 \cdot 10^6$	$2.18 \cdot 10^6$	–

A good similarity exists between the equivalent masses calculated from the mobility diagrams and from the modal profiles. The suggestion is, therefore, made that the measurements were performed with a favourable relative and absolute accuracy.

7 Discussion

The most striking result is the fact that the four-noded vertical vibration mode occurs at two different frequencies with different equivalent masses.

In this respect it is interesting to compare the measured results with the calculated natural frequencies and modal profiles, especially the four-noded vertical vibration mode. This is done in figure 9. The data of the calculations are from "Critical consideration of present hull vibrations analysis" by Ir. S. Hylarides, Report No. 144 S of the Neth. Ship Research Centre (to be published).

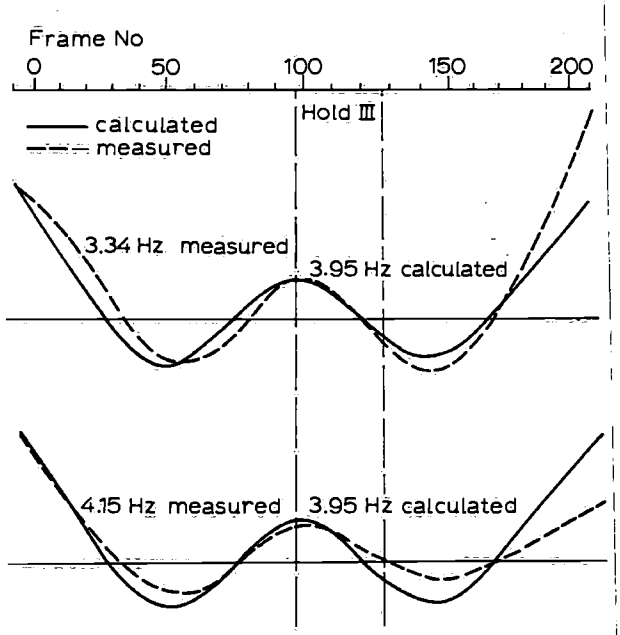

Fig. 9. Comparison of the measured and calculated four-noded vertical vibration mode.

In comparison to the calculated results the measurements show significantly larger amplitudes at 3.34 Hz from frame number 120. At 4.15 Hz the amplitudes are smaller. Larger amplitudes increase the equivalent mass and smaller amplitudes decrease the mass. In case a second mass-spring system is attached to the basic system, the occurrence of two resonant frequencies, the one smaller and the other larger than the natural frequency of the dynamic system, is typical. Without any doubt the secundary mass-spring system which causes the measured effect is the elasticity of the double-bottom, loaded with a part of the cargo. The measurement on the double-bottom in hold III and the calculation of the natural frequency of the bottom section point in the same direction. However, it may be decided from the modal profiles that the influence of the bottom section of hold II is even larger.

8 Conclusions

1. The equivalent masses calculated from the mobility diagram and from the modal profiles show good similarity.
2. The four-noded vertical vibration mode occurs at two different frequencies. The effect is caused by the double-bottom vibrations.
3. For accurate calculation of the natural frequencies of the hull at the vibration modes with four nodes and more, the double-bottom vibrations have to be taken into account.
4. The natural frequencies are greatly influenced by the loading conditions, because the natural frequency of the double-bottom is determined, among other factors, by the mass resting on it.

9 Evaluation of techniques of measurement

The techniques of measurement are accurate. In spite of the relatively large disturbancies caused by the propulsion system, the analysis of the exciter signals was successful. However, the bandwidth of the filter was 2 Hz constant, which is large for the frequency range under consideration.

The lack of usable results above 4.5 Hz is disappointing. It is unknown whether this lack is caused by a relatively large damping of the hull vibrations at a speed of 19–20 knots or by inadequate analysis of the signals. The effective bandwidth of the filter can be reduced by frequency transformation with the aid of a tape recorder. A frequency transformation with a factor of 8 and an effective bandwidth of 0.25 Hz will be a practical solution. Moreover, above 4.5 Hz better results can be expected if such measurements are carried out when the main engine is stopped.

Acknowledgement

The author wishes to express his thanks to Mr. Eradus and Mr. Geirnaert, who mounted the measuring equipment and did the practical work. Thanks are likewise due to the officers and crew of the m.v. "Koudekerk" for their co-operative attitude throughout the measurements.

Literature

1. Colloquium on Mechanical Impedance Methods for Mechanical Vibrations. A.S.M.E. Annual Meeting, New York, Dec. 2, 1958.
2. HARRIS, C. M. and C. E. CREDE, Shock and Vibration Handbook, Volume 1, 2 and 3. Mc. Graw-Hill Book Company Inc., New York, 1961.
3. THORN, R. P., The mobility method. Machine Design 1959, Dec. 10 and Dec. 24.
4. CHURCH, A. H., Simplified Vibration Analysis, Machine Design 1960, Febr. 18, March 3, March 17, March 31, April 14, April 28 and May 26.

Appendix A Tables

Table A-I. Calibration factors q of accelerometers in hold III.

measuring point	V/V per g $\times 10^{-6}$	at 5 V excitation and amplification factor 1,000 1 mV $\triangleq \ldots \cdot 10^{-3}$ m/sec^2
25	930	2.11
26	1992	0.985
27	1798	1.09
28	–	–
29	1941	1.01
30	2049	0.985
31	1100	1.78
32	1150	1.71
33	1150	1.71
34	1100	1,78
35	1150	1.71
36	1100	1.78

Table A-II. Calibration factors "acceleration" q of the 6 TNO accelerometers.

G_1 vert.	G_2 vert.	G_3 vert.	G_5 hor.	G_6 hor.	G_7 hor.
$200mg = 1.962$ m/sec$^2 \triangleq \ldots$ mV					
1420	1260	1570	1560	1490	1440
1430	1500	1515	1540	1490	1410
1420	1240	1610	1550	1460	1390
1430	1490	1585	1540	1470	1410
1420	1280	1575	1550	1440	–
1440	1500	1600	1550	1460	–
1440	1240	1580	1530	1440	–
1430	1450	1575	1530	1450	–
1.962 m/sec$^2 \triangleq \ldots$ mV averaged					
1428.75	1370.00	1576.25	1543.75	1462.50	1412.50
1 mV$\triangleq \ldots$ m/sec^2					
$1.37 \cdot 10^{-3}$	$1.43 \cdot 10^{-3}$	$1.24 \cdot 10^{-3}$	$1.27 \cdot 10^{-3}$	$1.34 \cdot 10^{-3}$	$1.39 \cdot 10^{-3}$
standard deviation $\sigma = \sqrt{\frac{(x-\bar{x})^2}{n-1}} \Big/ \bar{x}\,\%$					
0.6%	9.0%	1.8%	0.7%	1.4%	1.5%

Table A-III. Calibration factors "force" p for vertical excitation (excitation force vertical $= C\omega^2$ N).

$C_A = 87.845$		$C_C = 43.923$		$C_E = 20.415$		$C_H = 7.2663$	
frequency (Hz)	1 mV$\triangleq \ldots$ N	frequency (Hz)	1 mV$\triangleq \ldots$ N	frequency (Hz)	1 mV$\triangleq \ldots$ N	frequency (Hz)	1 mV$\triangleq \ldots$ N
1.33	57.48	2.55	53.57	4.26	54.40	6.42	51.09
1.39	55.09	2.59	54.78	4.34	52.52	6.50	51.33
1.42	55.22	2.77	53.16	4.44	53.04	6.58	51.59
1.45	54.98	2.79	51.09	4.51	53.97	6.71	50.49
1.50	56.56	2.88	52.09	4.59	53.20	6.76	50.87
1.62	55.33	2.92	52.79	4.66	51.69	6.92	51.40
1.74	54.54	2.96	52.72	4.78	52.68	7.05	52.68
1.89	53.30	3.00	52.88	4.91	51.95	7.22	53.40
1.98	52.45	3.03	52.87	5.00	51.51	7.33	53.32
2.22	53.57	3.09	53.57	5.11	51.44	7.59	53.85
2.39	51.77	3.14	56.23	5.20	52.05	7.77	53.42
2.44	51.75	3.37	54.28	5.26	51.37	7.89	53.06
2.46	52.62	3.61	53.71	5.45	51.64	8.07	51.84
2.72	57.82	4.00	52.51	5.55	51.86	8.14	52.95
2.81	53.32	4.20	52.90	5.68	50.67	8.48	51.29
averaged	54.39	averaged	53.38	averaged	52.26	averaged	52.17
σ	3.3%	σ	2.2%	σ	2.0%	σ	2.1%
σ'	0.9%	σ'	0.6%	σ'	0.5%	σ'	0.5%

$$\sigma = \sqrt{\frac{\Sigma(x-\bar{x})^2}{n-1}} \qquad \sigma' = \sqrt{\frac{\Sigma(x-\bar{x})^2}{n(n-1)}}$$

Table A-IV. Calibration factors "force" p for horizontal excitation (excitation force horizontal $C\omega^2$ N).

$C_B = 58.558$		$C_C = 43.923$		$C_E = 20.415$		$C_H = 7.2663$	
frequency (Hz)	1 mV△ ... N	frequency (Hz)	1 mV△ ... N	frequency (Hz)	1 mV△ ... N	frequency (Hz)	1 mV△ ... N
1.44	84.32	3.02	71.87	4.23	72.57	6.52	76.53
1.46	83.63	3.08	72.98	4.32	74.73	6.61	76.88
1.49	83.07	3.18	72.08	4.49	73.47	6.66	76.46
1.54	83.84	3.29	72.15	4.64	72.57	6.76	75.56
1.58	83.98	3.37	71.24	4.77	72.36	6.88	76.25
1.64	83.42	3.45	71.94	4.93	71.18	7.04	75.63
1.69	85.51	3.52	71.31	5.05	72.50	7.23	76.05
1.74	86.55	3.63	75.21	5.16	71.87	7.48	75.70
1.77	86.69	3.73	78.06	5.28	74.79	7.65	74.58
1.96	84.88	3.81	74.45	5.37	75.42	7.80	70.90
1.95	87.87	3.89	73.05	5.53	74.51	8.04	74.24
1.90	87.53	3.98	73.75	5.67	73.26	8.28	74.93
1.97	94.49	4.13	75.49	5.80	72.84	8.45	74.10
2.02	90.03	4.23	73.40	5.89	72.84	8.67	76.95
2.07	90.38	4.31	74.31	6.01	74.03	9.00	76.74
averaged	86.41	averaged	73.40	averaged	73.26	averaged	75.42
$\bar{\sigma}$	3.7%	σ	2.3%	σ	1.6%	σ	2.4%
σ'	1.0%	σ'	0.6%	σ'	0.4%	σ'	0.5%

Table A-V. Abstract from the meteo reports at 12.00 a.m.

			wind			ship		waves			swell		
aug. 1967	temp. air	pressure	direction	speed	beaufort	course	speed	direction	period	height	direction	period	height
	°C	millibar	grades	knots		grades	knots	grades	s	m	grades	s	m
6	20.0	1013.2	080	02	1	208/197	19–21	080	⩽ 5	¼	080	⩽ 5	¾–1¼
7	21.1	1013.9	290	05	2	197	19–21	290	⩽ 5	¼– ¾	350	⩽ 5	¾–1¼
8	22.9	1011.7	020	16	4–5	197	19–21	020	6–7	¾–1¼	030	6–7	1¼–1¾
9	22.9	1009.2	030	19	5	197	19–21	030	8–9	1¾–2¼	020	8–9	1¾–2¼
10	27.0	1007.9	030	09	3	180	19–21	030	⩽ 5	¼– ¾	220	6–7	¾–1¼
11	25.3	1010.6	160	12	3–4	143	19–21	160	⩽ 5	1¼–1¾	160	8–9	1¾–2¼
12	22.8	1013.0	170	08	2–3	143	19–21	170	⩽ 5	¾–1¼	160	6–7	1¼–1¾
13	23.0	1010.8	140	16	4–5	143	19–21	140	6–7	1¼–1¾	140	6–7	2¼–2¾
14	20.4	1013.4	140	13	4	143	19–21	140	6–7	1¼–1¾	140	10–11	2¼–2¾
15	18.2	1016.4	140	13	4	143	16–18	140	6–7	1¼–1¾	150	8–9	2¾–3¼
16	17.0	1019.9	140	12	3–4	140	19–21	140	6–7	1¼–1¾	140	8–9	2¼–2¾
17		1024.2	170	22	5–6	139	19–21	170	6–7	¼– ¾	170	10–11	3¼–3¾

Appendix B Diagrammes

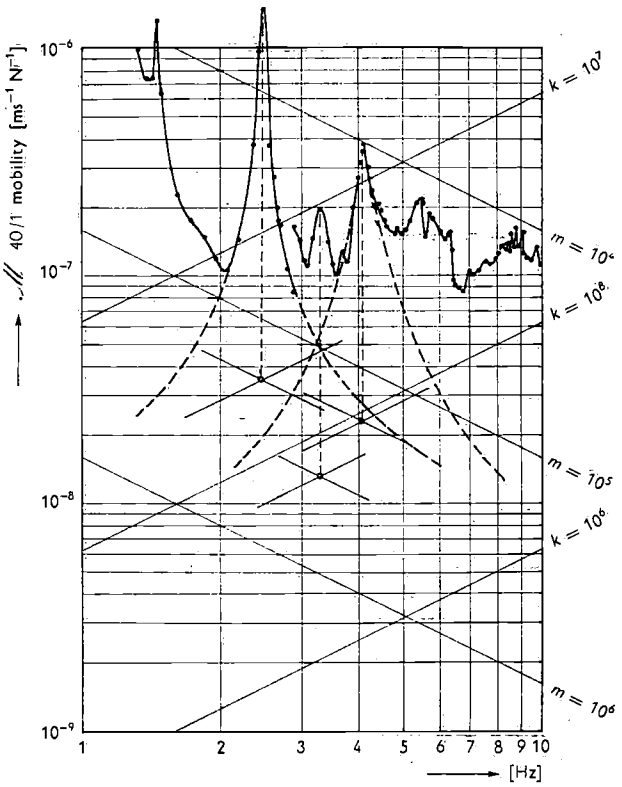

Diagram B-1. Measuring point 1.
vertical excitation
vertical response

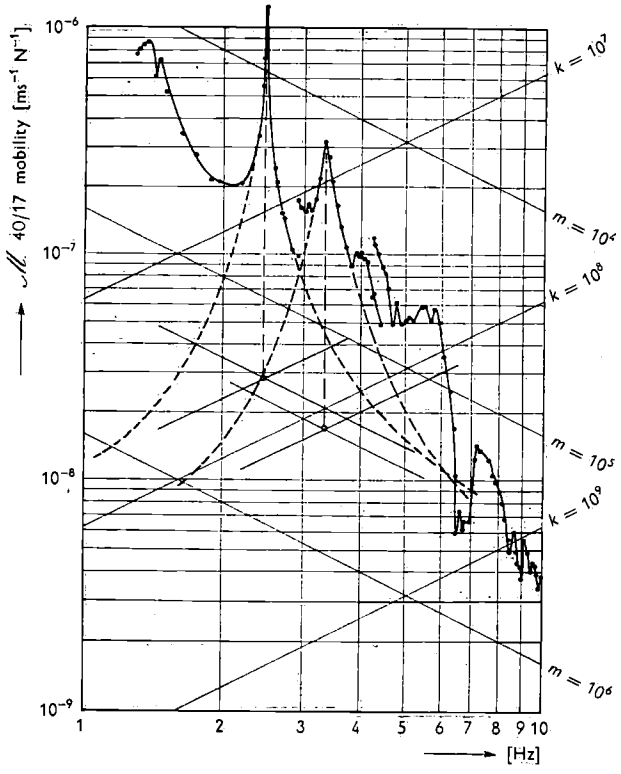

Diagram B-2. Measuring point 17.
vertical excitation
vertical response

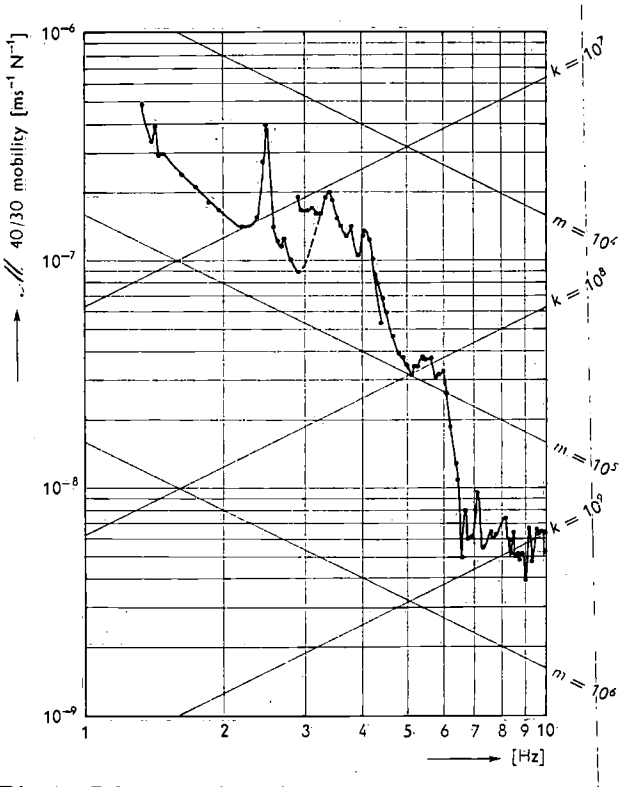

Diagram B-3. Measuring point 30.
vertical excitation
vertical response

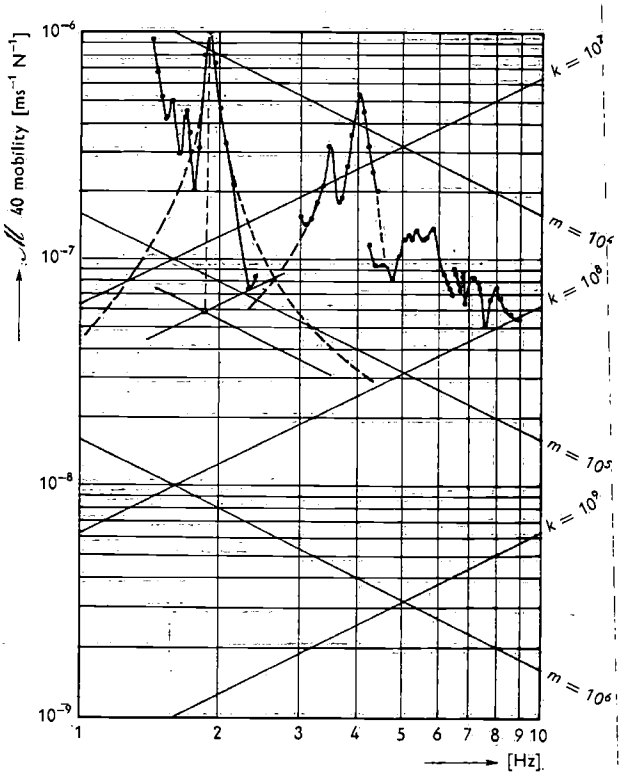

Diagram B-4. Measuring point 40.
horizontal athwartships excitation
horizontal athwartships response

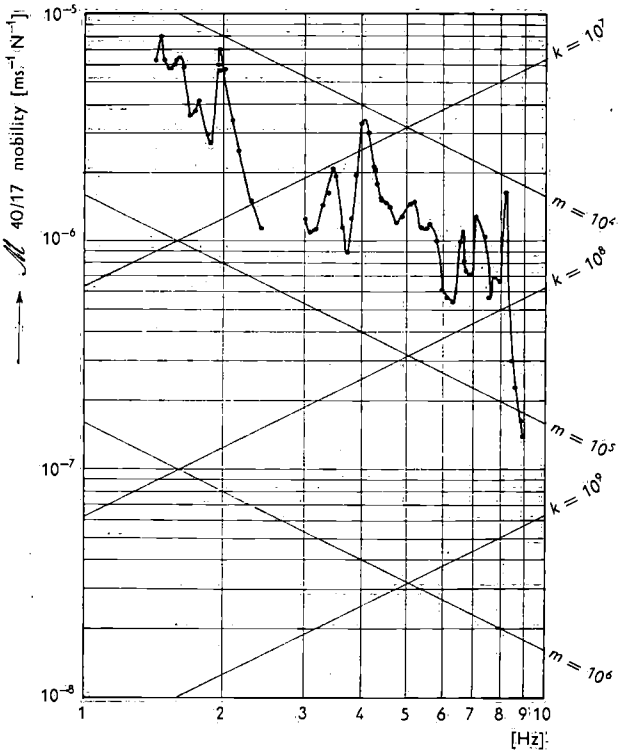

Diagram B-5. Measuring point 17.
horizontal athwartships excitation
horizontal athwartships response

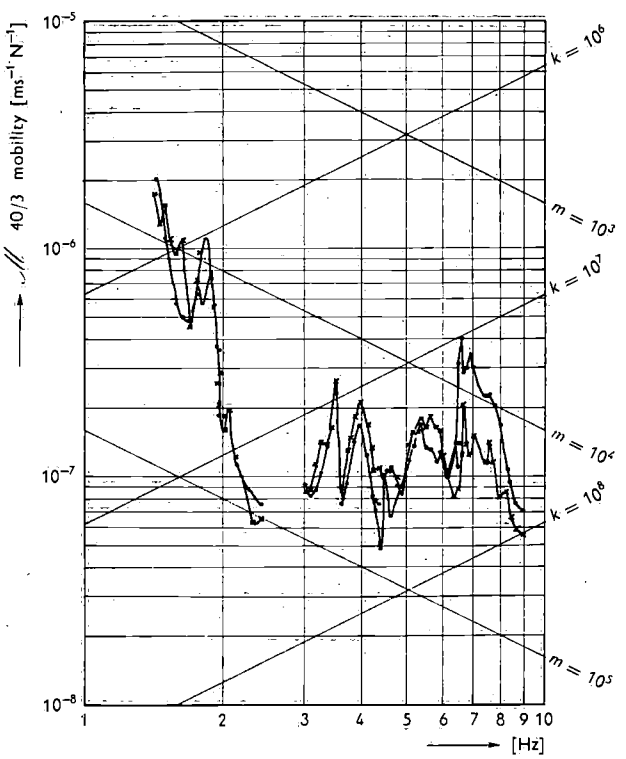

Diagram B-6. Measuring point 3 (·) and 3a (×).
horizontal athwartships excitation
vertical response

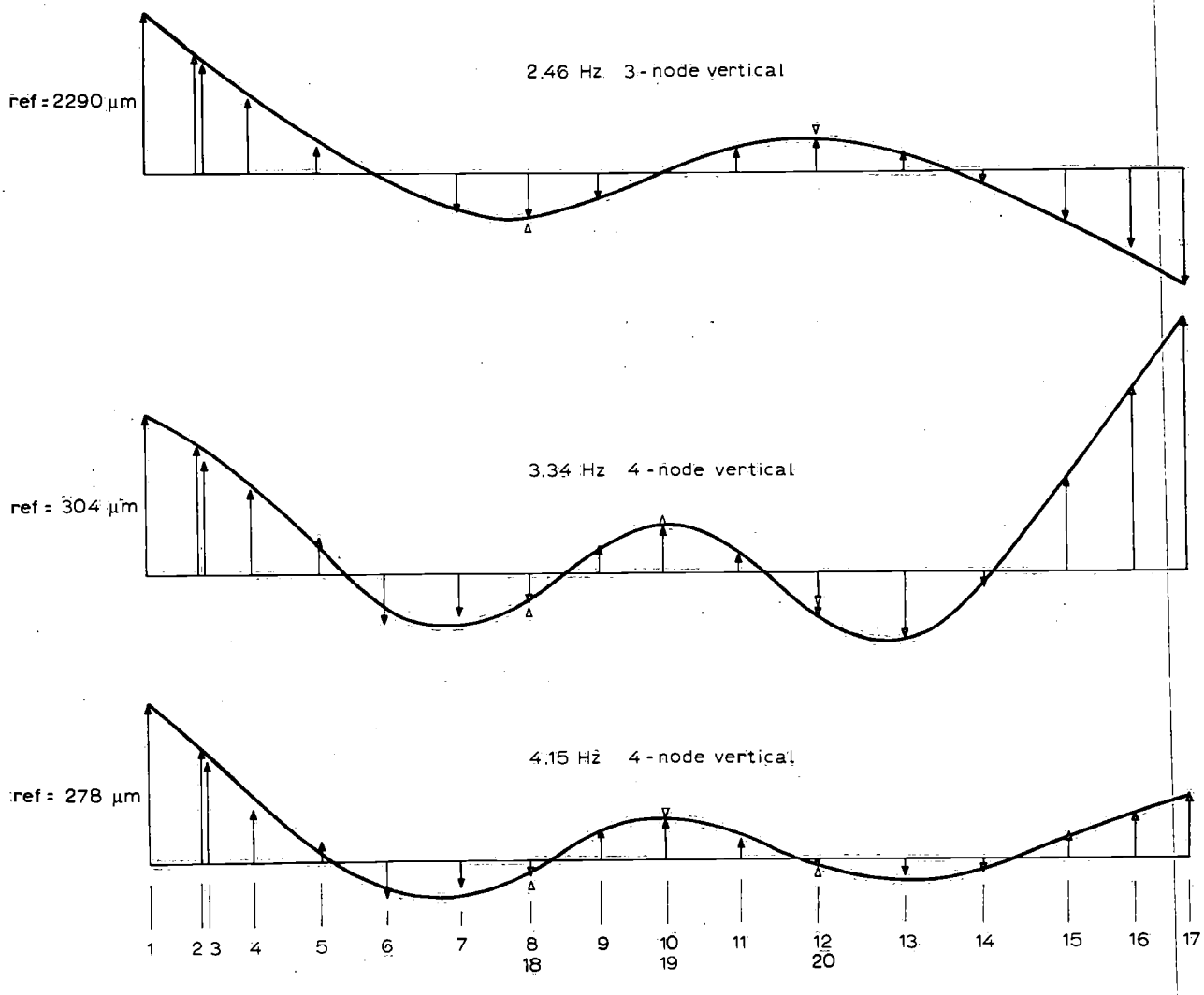

Diagram B-7. Vertical modal profiles.

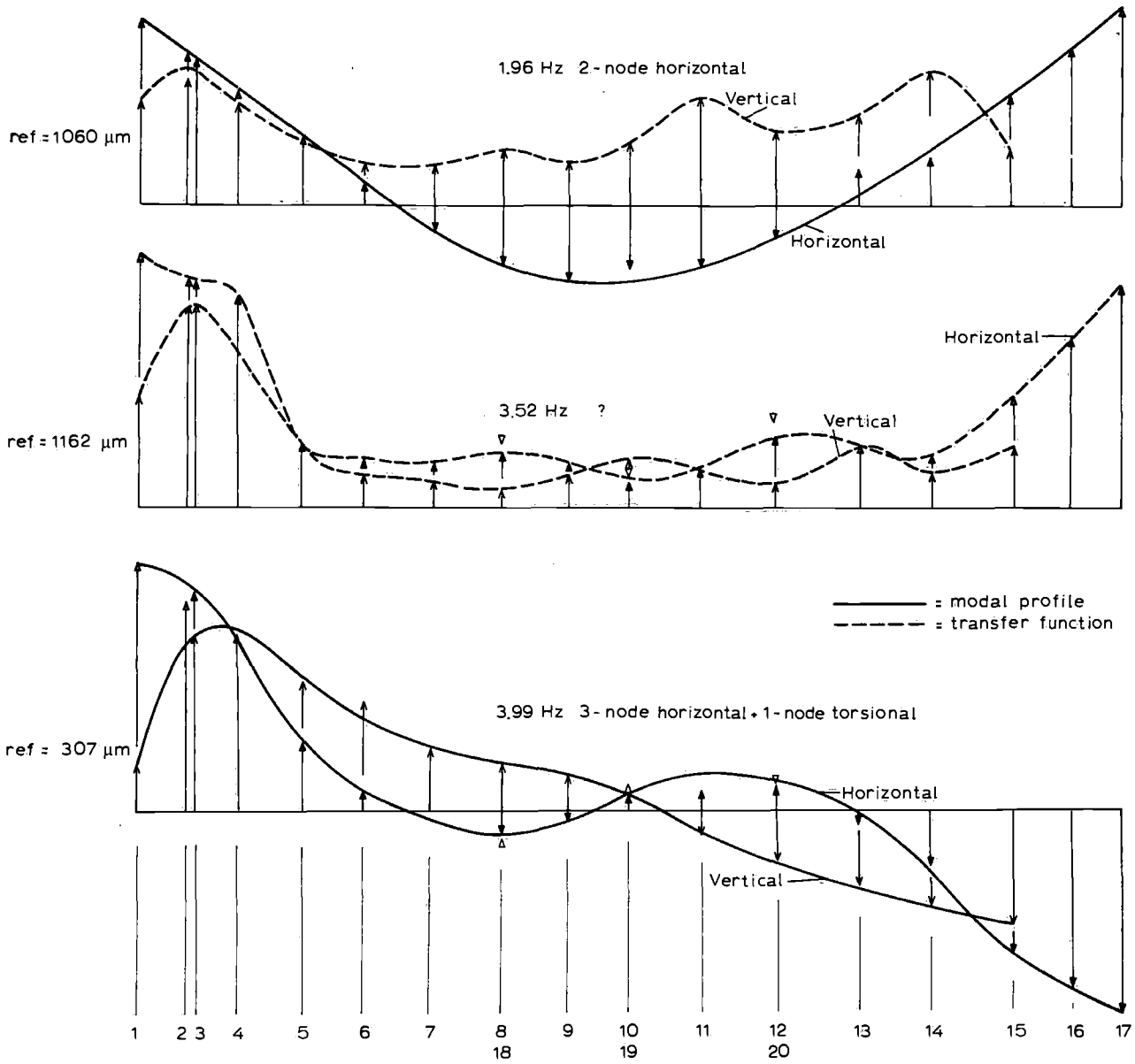

Diagram B-8. Horizontal and vertical modal profiles and transfer functions at horizontal excitation.

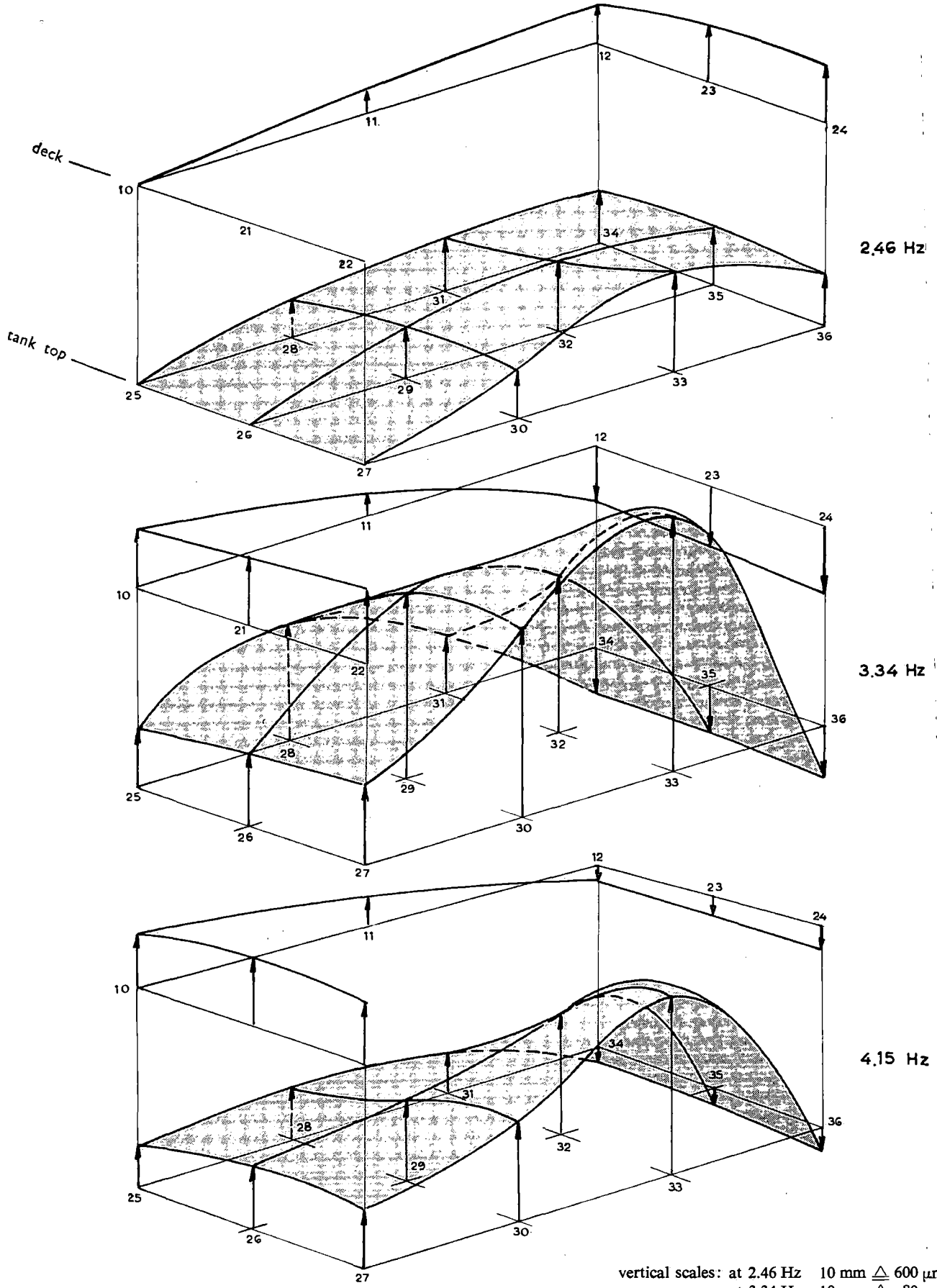

vertical scales: at 2.46 Hz 10 mm △ 600 μm
at 3.34 Hz 10 mm △ 80 μm
at 4.15 Hz 10 mm △ 73 μm

Diagram B-9. Vibration modes double bottom hold III.

Appendix C

I. *Determination of the mobilities of spring, mass and damper*

In the mobility method, the dynamic characteristics of an element or of any combination of elements are expressed by the relationship between the force through the element on the one hand and the displacement across the element on the other hand, using algebraic equations with complex numbers.

The following magnitudes are most commonly used:

Mechanical impedance	$Z = F/v$
Mobility	$\mathcal{M} = v/F$
Dynamic modulus	$D = F/x$
Receptance	$R = x/F$

These magnitudes are expressed by complex numbers; besides an amplitude relation there is also a phase relation between the force F and the velocity v or displacement x.

If the force and the velocity relate to the same point of the system, the expression "driving-point mobility" is used. If the force and the velocity are not measured at the same point, the expression "transfer mobility" is used.

Using the concept of mobility has the advantage that a mobility diagram looks like a classical amplification curve.

The mobilities of the three simplest dynamic systems, viz. linear damper, ideal mass and linear spring, are calculated below.

a. Damper

To a linear damper applies:

$$F_1 = c(v_1 - v_2)$$

If, on one side, the damper is attached to a fixed point:

$$v_2 = 0 \quad \text{and} \quad F_1 = cv_1$$

or

$$\frac{v_1}{F_1} = \mathcal{M}_c = \frac{1}{c}$$

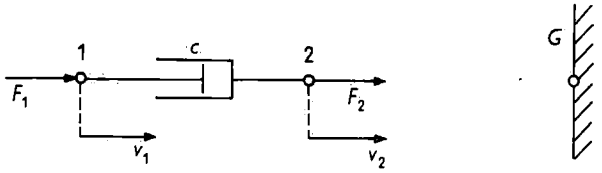

Fig. C-1. Dynamic system of linear damper.

b. Mass

To the ideal mass applies:

$$F_1 = m \cdot \ddot{x}_1$$

To the sinusoidal excitation applies:

$$F_1 = F_0 \cdot e^{j\omega t}$$

$$\ddot{x}_1 = \frac{F_0 \cdot e^{j\omega t}}{m}$$

Through integration is obtained:

$$\dot{x}_1 = v_1 = \frac{F_0 \cdot e^{j\omega t}}{j\omega m}$$

and

$$\frac{v_1}{F_1} = \frac{F_0 \cdot e^{j\omega t}}{j\omega m \cdot F_0 e^{j\omega t}} = \frac{1}{j\omega m}$$

$$\mathcal{M}_m = \frac{1}{j\omega m}$$

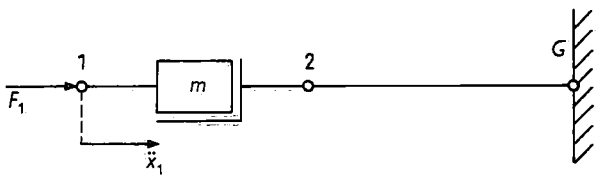

Fig. C-2. Dynamic system of ideal mass.

c. Spring

To the linear spring applies:

$$F_1 = k(x_1 - x_2)$$

If the spring is attached to a fixed point:

$$F_1 = kx_1$$

To the sinusoidal excitation applies:

$$F_1 = F_0 \cdot e^{j\omega t}$$

$$x_1 = \frac{F_0 \cdot e^{j\omega t}}{k}$$

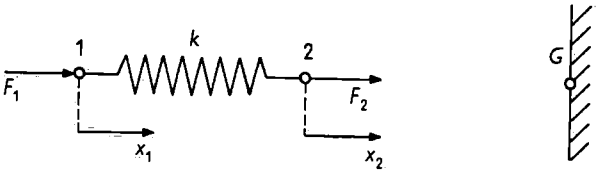

Fig. C-3. Dynamic system of linear spring.

Differentiation results in:

$$\dot{x}_1 = \frac{j\omega F_0 \cdot e^{j\omega t}}{k}$$

and

$$\frac{\dot{x}_1}{F_1} = \frac{j\omega}{k}$$

$$\mathcal{M}_k = \frac{j\omega}{k}$$

The mobilities of the three basic systems are presented graphically in fig. C-4.

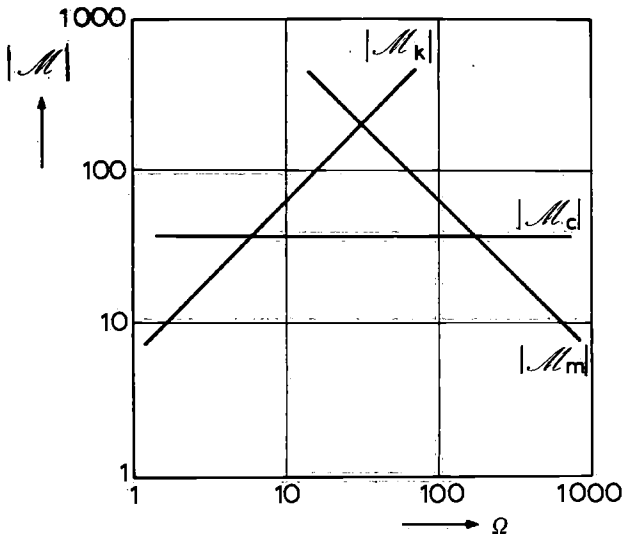

Fig. C-4. Mobilities of spring (k), damper (c) and mass (m). (logarithmic scales)

II. *Determination of the mobility of a single degree-of-freedom system*

Every dynamic system can be composed of a network of masses, springs and dampers, or, in more general terms, a network of elements, having certain mobilities or impedances.

In parallel arrangement of elements, the same velocity acts through all elements. Hence, the total impedance is the sum of the impedances of the elements:

$$Z = \frac{F}{v} = \frac{F_1}{v} + \frac{F_2}{v} + \ldots = \sum_i \frac{F_i}{v} = \sum_i Z_i$$

For the series arrangement, this applies to the mobilities, since the same force then acts through all elements.

$$\mathcal{M} = \frac{v}{F} = \frac{v_1}{F} + \frac{v_2}{F} + \ldots = \sum_i \frac{v_i}{F} = \sum_i \mathcal{M}_i$$

So, at series arrangements:

$$\mathcal{M} = \sum \mathcal{M}_i$$

At parallel arrangements:

$$Z = \sum Z_i \quad \text{or} \quad \mathcal{M} = \frac{1}{\sum 1/\mathcal{M}_i}$$

As an example we take a simple linear mass-spring system with damping. The mass is excited by a force F_1. Fig. C-5 shows the mechanical system in outline and the equivalent network. The mobility in the excitation point is:

$$\mathcal{M}_{11} = \frac{F_1}{v_1} = \frac{\mathcal{M}_1\mathcal{M}_2\mathcal{M}_3}{\mathcal{M}_1\mathcal{M}_2 + \mathcal{M}_2\mathcal{M}_3 + \mathcal{M}_1\mathcal{M}_3}$$

where:

$$\mathcal{M}_1 = \mathcal{M}_m = -j/\omega m$$

$$\mathcal{M}_2 = \mathcal{M}_k = j\omega/k$$

$$\mathcal{M}_3 = \mathcal{M}_c = 1/c$$

and

$$\mathcal{M}_{11} = \frac{1/mck}{1/mk + j\omega/ck - j/\omega mc}$$

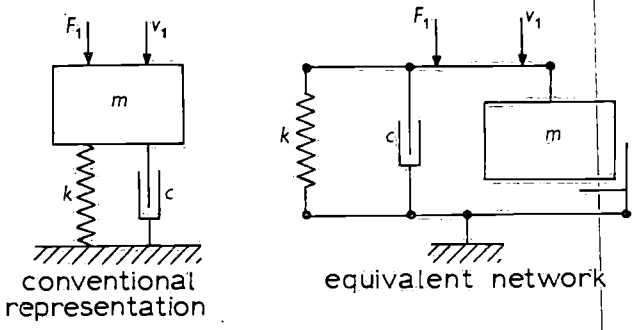

Fig. C-5. One degree-of-freedom system.

Numerator and denominator are multiplied by $j\omega mc$. Further new magnitudes are introduced, viz.

$$\Omega = \omega/\omega_0 \qquad \omega_0 = \sqrt{k/m}$$

$$\beta = c/c_c \qquad c_c = 2\sqrt{km}$$

This results in:

$$\mathcal{M}_{11} = \frac{j\omega/k}{(1-\Omega^2) + j2\Omega\beta}$$

The absolute value (modulus) of $\mathcal{M}_{11}$ is:

$$|\mathcal{M}_{11}| = \frac{\omega/k}{\sqrt{(1-\Omega^2)^2 + 4\beta^2\Omega^2}}$$

This equation is shown in a graph in fig. C-6.

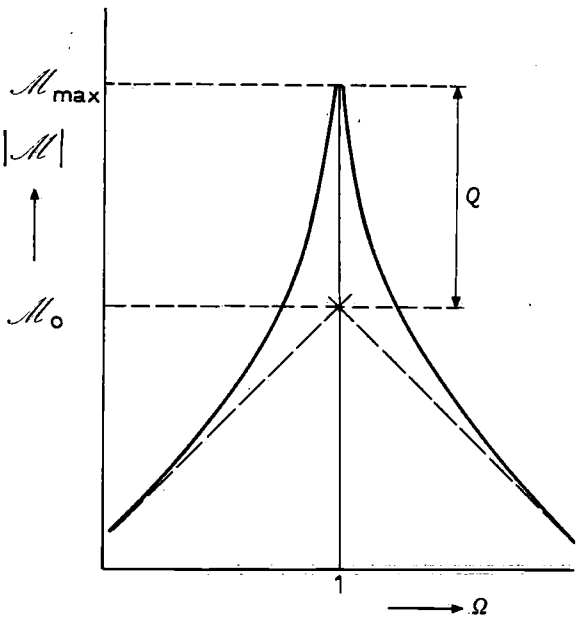

Fig. C-6. Mobility diagram of a one-degree-of-freedom system. (logarithmic scales)

If ω represents small values this results in:

$$|\mathcal{M}_{11}| = \frac{\omega}{k} \qquad \omega \to 0$$

This is the mobility of the spring of the system. The system is "spring-controlled" in case of a low frequency.

If ω represents large values, this results in:

$$|\mathcal{M}_{11}| = \frac{1}{\omega m} \qquad \omega \to \infty$$

With high frequencies, the system is "mass-controlled". With resonance, $\omega = \omega_0$ ($\Omega = 1$) and

$$|\mathcal{M}_{11}| = \frac{\omega_0}{2\beta k} = \frac{1}{c}$$

the system is "damper-controlled".

III. *Computing the damping from the width of the resonance peak*

$$|\mathcal{M}|_{max} = \frac{1}{2\beta \cdot \sqrt{km}}$$

Introducing p:

$$|\mathcal{M}| = p \cdot |\mathcal{M}|_{max}$$

with $p < 1$

$$|\mathcal{M}| = \frac{p}{2\beta \cdot \sqrt{km}}$$

so that

$$\frac{p}{2\beta} = \frac{\Omega}{\sqrt{(1-\Omega^2)^2 + 4\beta^2\Omega^2}}$$

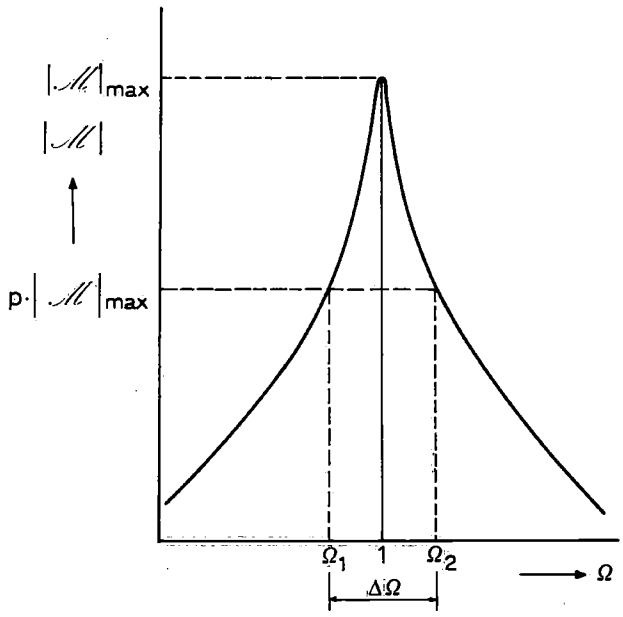

Fig. C-7. Method of determining β from the resonance curve.

Squaring gives the following equation:

$$4\beta^2(p^2-1)\cdot\Omega^2 + p^2(1-\Omega^2)^2 = 0 \qquad (1)$$

If we say that

$$\Omega = 1+\varepsilon, \quad \text{where } \varepsilon \ll 1 \qquad (2)$$

and introduce this in (1), we find that:

$$4\beta^2(p^2-1)\cdot(1+2\varepsilon+\varepsilon^2) + 4p^2\varepsilon^2 = 0$$

It is permissible to neglect certain factors if we also assume that $\beta^2 \ll 1$; then:

$$\beta^2(p^2-1) + p^2\varepsilon^2 = 0,$$

or:

$$\varepsilon^2 = \beta^2(1/p^2-1) \quad \text{and} \quad \varepsilon = \pm\beta\sqrt{1/p^2-1}$$

Substitution in (2) then yields:

$$\Omega_{2,1} = 1 \pm \beta\sqrt{1/p^2-1}$$

$$\Delta\Omega = \Omega_2 - \Omega_1 = \frac{\Delta\omega}{\omega_0} = 2\beta\sqrt{1/p^2-1}$$

PUBLICATIONS OF THE NETHERLANDS SHIP RESEARCH CENTRE TNO

PUBLISHED AFTER 1963 (LIST OF EARLIER PUBLICATIONS AVAILABLE ON REQUEST)
PRICE PER COPY DFL. 10,—

M = engineering department S = shipbuilding department C = corrosion and antifouling department

Reports

57 M Determination of the dynamic properties and propeller excited vibrations of a special ship stern arrangement. R. Wereldsma, 1964.
58 S Numerical calculation of vertical hull vibrations of ships by discretizing the vibration system, J. de Vries, 1964.
59 M Controllable pitch propellers, their suitability and economy for large sea-going ships propelled by conventional, directly coupled engines. C. Kapsenberg, 1964.
60 S Natural frequencies of free vertical ship vibrations. C. B. Vreugdenhil, 1964.
61 S The distribution of the hydrodynamic forces on a heaving and pitching shipmodel in still water. J. Gerritsma and W. Beukelman, 1964.
62 C The mode of action of anti-fouling paints: Interaction between anti-fouling paints and sea water. A. M. van Londen, 1964.
63 M Corrosion in exhaust driven turbochargers on marine diesel engines using heavy fuels. R. W. Stuart Mitchell and V. A. Ogale, 1965.
64 C Barnacle fouling on aged anti-fouling paints; a survey of pertinent literature and some recent observations. P. de Wolf, 1964.
65 S The lateral damping and added mass of a horizontally oscillating shipmodel. G. van Leeuwen, 1964.
66 S Investigations into the strength of ships' derricks. Part I. F. X. P. Soejadi, 1965.
67 S Heat-transfer in cargotanks of a 50,000 DWT tanker. D. J. van der Heeden and L. L. Mulder, 1965.
68 M Guide to the application of method for calculation of cylinder liner temperatures in diesel engines. H. W. van Tijen, 1965.
69 M Stress measurements on a propeller model for a 42,000 DWT tanker. R. Wereldsma, 1965.
70 M Experiments on vibrating propeller models. R. Wereldsma, 1965.
71 S Research on bulbous bow ships. Part II. A. Still water performance of a 24,000 DWT bulkcarrier with a large bulbous bow. W. P. A. van Lammeren and J. J. Muntjewerf, 1965.
72 S Research on bulbous bow ships. Part II. B. Behaviour of a 24,000 DWT bulkcarrier with a large bulbous bow in a seaway. W. P. A. van Lammeren and F. V. A. Pangalila, 1965.
73 S Stress and strain distribution in a vertically corrugated bulkhead. H. E. Jaeger and P. A. van Katwijk, 1965.
74 S Research on bulbous bow ships. Part I. A. Still water investigations into bulbous bow forms for a fast cargo liner. W. P. A. van Lammeren and R. Wahab, 1965.
75 S Hull vibrations of the cargo-passenger motor ship "Oranje Nassau", W. van Horssen, 1965.
76 S Research on bulbous bow ships. Part I. B. The behaviour of a fast cargo liner with a conventional and with a bulbous bow in a seaway. R. Wahab, 1965.
77 M Comparative shipboard measurements of surface temperatures and surface corrosion in air cooled and water cooled turbine outlet casings of exhaust driven marine diesel engine turbochargers. R. W. Stuart Mitchell and V. A. Ogale, 1965.
78 M Stern tube vibration measurements of a cargo ship with special afterbody. R. Wereldsma, 1965.
79 C The pre-treatment of ship plates: A comparative investigation on some pre-treatment methods in use in the shipbuilding industry. A. M. van Londen, 1965.
80 C The pre-treatment of ship plates: A practical investigation into the influence of different working procedures in over-coating zinc rich epoxy-resin based pre-construction primers. A. M. van Londen and W. Mulder, 1965.
81 S The performance of U-tanks as a passive anti-rolling device. C. Stigter, 1966.
82 S Low-cycle fatigue of steel structures. J. J. W. Nibbering and J. van Lint, 1966.
83 S Roll damping by free surface tanks. J. J. van den Bosch and J. H. Vugts, 1966.
84 S Behaviour of a ship in a seaway. J. Gerritsma, 1966.
85 S Brittle fracture of full scale structures damaged by fatigue. J. J. W. Nibbering, J. van Lint and R. T. van Leeuwen, 1966.
86 M Theoretical evaluation of heat transfer in dry cargo ship's tanks using thermal oil as a heat transfer medium. D. J. van der Heeden, 1966.
87 S Model experiments on sound transmission from engineroom to accommodation in motorships. J. H. Janssen, 1966.
88 S Pitch and heave with fixed and controlled bow fins. J. H. Vugts, 1966.
89 S Estimation of the natural frequencies of a ship's double bottom by means of a sandwich theory. S. Hylarides, 1967.
90 S Computation of pitch and heave motions for arbitrary ship forms. W. E. Smith, 1967.
91 M Corrosion in exhaust driven turbochargers on marine diesel engines using heavy fuels. R. W. Stuart Mitchell, A. J. M. S. van Montfoort and V. A. Ogale, 1967.
92 M Residual fuel treatment on board ship. Part II. Comparative cylinder wear measurements on a laboratory diesel engine using filtered or centrifuged residual fuel. A. de Mooy, M. Verwoest and G. G. van der Meulen, 1967.
93 C Cost relations of the treatments of ship hulls and the fuel consumption of ships. H. J. Lageveen-van Kuijk, 1967.
94 C Optimum conditions for blast cleaning of steel plate. J. Remmelts, 1967.
95 M Residual fuel treatment on board ship. Part I. The effect of centrifuging, filtering and homogenizing on the unsolubles in residual fuel. M. Verwoest and F. J. Colon, 1967.
96 S Analysis of the modified strip theory for the calculation of ship motions and wave bending moments. J. Gerritsma and W. Beukelman, 1967.
97 S On the efficacy of two different roll-damping tanks. J. Bootsma and J. J. van den Bosch, 1967.
98 S Equation of motion coefficients for a pitching and heaving destroyer model. W. E. Smith, 1967.
99 S The manoeuvrability of ships on a straight course. J. P. Hooft, 1967.
100 S Amidships forces and moments on a $C_B = 0.80$ "Series 60" model in waves from various directions. R. Wahab, 1967.
101 C Optimum conditions for blast cleaning of steel plate. Conclusion. J. Remmelts, 1967.
102 M The axial stiffness of marine diesel engine crankshafts. Part I. Comparison between the results of full scale measurements and those of calculations according to published formulae. N. J. Visser, 1967.
103 M The axial stiffness of marine diesel engine crankshafts. Part II. Theory and results of scale model measurements and comparison with published formulae. C. A. M. van der Linden, 1967.
104 M Marine diesel engine exhaust noise. Part I. A mathematical model. J. H. Janssen, 1967.
105 M Marine diesel engine exhaust noise. Part II. Scale models of exhaust systems. J. Buiten and J. H. Janssen, 1968.
106 M Marine diesel engine exhaust noise. Part III. Exhaust sound criteria for bridge wings. J. H. Janssen en J. Buiten, 1967.
107 S Ship vibration analysis by finite element technique. Part I. General review and application to simple structures, statically loaded. S. Hylarides, 1967.
108 M Marine refrigeration engineering. Part I. Testing of a decentralised refrigerating installation. J. A. Knobbout and R. W. J. Kouffeld, 1967.
109 S A comparative study on four different passive roll damping tanks. Part I. J. H. Vugts, 1968.
110 S Strain, stress and flexure of two corrugated and one plane bulkhead subjected to a lateral, distributed load. H. E. Jaeger and P. A. van Katwijk, 1968.
111 M Experimental evaluation of heat transfer in a dry-cargo ships' tank, using thermal oil as a heat transfer medium. D. J. van der Heeden, 1968.
112 S The hydrodynamic coefficients for swaying, heaving and rolling cylinders in a free surface. J. H. Vugts, 1968.
113 M Marine refrigeration engineering. Part II. Some results of testing a decentralised marine refrigerating unit with R 502. J. A. Knobbout and C. B. Colenbrander, 1968.
114 S The steering of a ship during the stopping manoeuvre. J. P. Hooft, 1969.
115 S Cylinder motions in beam waves. J. H. Vugts, 1968.